Quantum tomography for arbitrary single-photon polarization-path states

J. L. Montenegro Ferreira [*] and Bertúlio de Lima Bernardo [†]

Departamento de Física, Universidade Federal da Paraíba, 58051-900 João Pessoa, Paraíba, Brazil

Quantum state tomography (QST), the process through which the density matrix of a quantum system is characterized from measurements of specific observables, is a fundamental pillar in the fields of quantum information and computation. In this work, we propose a simple QST method to reconstruct the density matrix of two qubits encoded in the polarization and path degrees of freedom of a single photon, which can be realized with a single linear-optical setup. We demonstrate that the density matrix can be fully described in terms of the Stokes parameters related to the two possible paths of the photon, together with a quantum version of the two-point Stokes parameters introduced here. Our findings put forward photonic circuits for the investigation of the dynamics of open quantum systems.

I. INTRODUCTION

With the advent of quantum information theory we learned that entanglement is an essential resource for many important tasks, such as quantum communication [1], quantum computation [2], quantum cryptography [3], and teleportation [4]. This fact has led to an intense search for ways to create and characterize entanglement in many different physical architectures, among which photons occupy a special place due to their capacity to carry information for long distances [5]. Notably, different degrees of freedom (DOF) can be used to entangle photons, including position, linear momentum, polarization, orbital angular momentum, frequency, and time-bin [6–8]. Nevertheless, entanglement can also be created between the different DOF of a single photon, which provides an alternative way to achieve high-dimensional entangled states over the use of multiple photons entangled in a single DOF [9].

In order to benefit from the valuable resources extractable from quantum states, besides the physical implementation, we also need to be able to control, measure, and characterize them. The process of reconstruction of a quantum state from measurements made on an ensemble of identical systems is called quantum state tomography (QST) [10–12]. The idea is to process the outcomes obtained from a complete set of observables to identify all elements of the density matrix of the system. To characterize an N-qubit state, measurements of 2^{2N} different observables are required [13]. Evidently, this exponential relation sets a limit on the feasibility of experimental realizations of QST with correlated many-body systems. Although this fact, an alternative platform, which has not been much explored, is the application of QST to high-dimension states encoded in different DOF of the same particle. Some exceptions are the studies of single photons entangled in

polarization and time and single neutrons entangled in spin and path [9,14].

In this work, we propose an experimental setup to realize QST for an arbitrary polarization-path state of a single photon, which encodes two qubits of information. The scheme is fundamentally based on the composition of a two-path interferometer and a set of four conveniently distributed measurers of Stokes parameters. The tomographic protocol demands only a single arrangement of linear optical devices, in the sense that one does not need to modify the experimental setup in order to measure all necessary observables. In what concerns our theoretical approach, besides the well-known one-point Stokes parameters, we introduce a quantum-mechanical version of the two-point Stokes parameters, a concept so far only established for classical optical fields [15]. In fact, the polarization-path density matrix is fully reconstructed on the basis of the quantum counterparts of the one- and two-point Stokes parameters, which we call one-path Stokes parameters (OPSPs) and two-path Stokes parameters (TPSPs), respectively.

The paper is organized as follows. First, we outline the quantum description of the OPSPs and propose a similar treatment for the TPSPs. Then, we use the results to demonstrate a QST method to reconstruct an arbitrary polarization-path state of a single photon. Finally, we present our conclusions and discuss how our QST method could be employed as a tool in the study of the dynamics of open single- and two-qubit systems with quantum optical experiments.

II. ONE- AND TWO-PATH STOKES PARAMETERS: A QUANTUM-MECHANICAL VIEWPOINT

Suppose that photons from an ensemble propagate one at a time through two possible paths 0 and 1 whose states are defined as $|0\rangle$ and $|1\rangle$, and the polarization is described in terms of the horizontal and vertical states, $|H\rangle$ and $|V\rangle$. In this case, the polarization and path properties of the photons can be jointly described in terms of the polarization-path density

*lukas.montenegrof@gmail.com
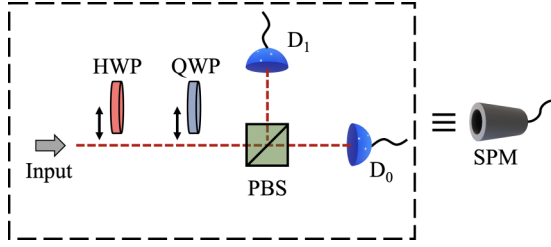†bertulio.fisica@gmail.com

FIG. 1. Experimental setup to measure the OPSPs. Photons with arbitrary polarization propagate toward the polarizing beam splitter (PBS). The parameter s_0 is found through the sum of the signals of the photodetectors D_0 and D_1. The other parameters are assessed through the difference of the signals: s_1 without the wave plates, s_2 only with the half-wave plate (HWP), and s_2 only with the quarter-wave plate (QWP). This apparatus is identified as a Stokes parameter measurer (SPM).

matrix [16],

$$\hat{\rho} = \begin{pmatrix} \rho_{11} & \rho_{12} & \rho_{13} & \rho_{14} \\ \rho_{21} & \rho_{22} & \rho_{23} & \rho_{24} \\ \rho_{31} & \rho_{32} & \rho_{33} & \rho_{34} \\ \rho_{41} & \rho_{42} & \rho_{43} & \rho_{44,} \end{pmatrix}, \quad (1)$$

which is written in the basis $\{|H, 0\rangle ; |H, 1\rangle ; |V, 0\rangle ; |V, 1\rangle\}$. In this framework, we can use the OPSPs to characterize the polarization of the photons in each path. From a quantum-mechanical viewpoint, these parameters are given by the ensemble average of the Pauli operators [13,16,17]. As such, the OPSPs for the photons that propagate through path 0 are given by

$$s_0^{(0)} = \mathrm{Tr}[(|H, 0\rangle \langle H, 0| + |V, 0\rangle \langle V, 0|)\hat{\rho}] = \rho_{11} + \rho_{33}, \quad (2a)$$

$$s_1^{(0)} = \mathrm{Tr}[(|H, 0\rangle \langle H, 0| - |V, 0\rangle \langle V, 0|)\hat{\rho}] = \rho_{11} - \rho_{33}, \quad (2b)$$

$$s_2^{(0)} = \mathrm{Tr}[(|H, 0\rangle \langle V, 0| + |V, 0\rangle \langle H, 0|)\hat{\rho}] = \rho_{13} + \rho_{31}, \quad (2c)$$

$$s_3^{(0)} = i\{\mathrm{Tr}[(|V, 0\rangle \langle H, 0| - |H, 0\rangle \langle V, 0|)\hat{\rho}]\} = i(\rho_{13} - \rho_{31}), \quad (2d)$$

where $\mathrm{Tr}[.]$ denotes the trace operation. Similarly, the polarization of the photons that propagate through path 1 is described by the corresponding OPSPs:

$$s_0^{(1)} = \mathrm{Tr}[(|H, 1\rangle \langle H, 1| + |V, 1\rangle \langle V, 1|)\hat{\rho}] = \rho_{22} + \rho_{44}, \quad (3a)$$

$$s_1^{(1)} = \mathrm{Tr}[(|H, 1\rangle \langle H, 1| - |V, 1\rangle \langle V, 1|)\hat{\rho}] = \rho_{22} - \rho_{44}, \quad (3b)$$

$$s_2^{(1)} = \mathrm{Tr}[(|H, 1\rangle \langle V, 1| + |V, 1\rangle \langle H, 1|)\hat{\rho}] = \rho_{24} + \rho_{42}, \quad (3c)$$

$$s_3^{(1)} = i\{\mathrm{Tr}[(|V, 1\rangle \langle H, 1| - |H, 1\rangle \langle V, 1|)\hat{\rho}]\} = i(\rho_{24} - \rho_{42}). \quad (3d)$$

From Eqs. (2a) to (3d) we observe that 8 out of the 16 entries of the polarization-path density matrix of Eq. (1) are sufficient to fully characterize the polarization of the photons propagating in each path.

The experimental setup to measure the OPSPs is shown in Fig. 1 (see also Refs. [18,19]). It consists of a polarizing beam-splitter (PBS), which transmits $|H\rangle$ and reflects $|V\rangle$ states; a half-wave plate (HWP); a quarter-wave plate (QWP); and two photodetectors D_0 and D_1. The parameter s_0 is simply

given by the sum of the number of photons registered in the photodetectors, independent of whether the wave plates are introduced along the optical path or not, divided by the number of input photons, $s_0 = (N_0 + N_1)/N_{\mathrm{in}}$. The parameters s_1, s_2, and s_3 are given by the difference between the signals registered by D_0 and D_1 divided by the number of input photons, $s_k = (N_0 - N_1)/N_{\mathrm{in}}$, with $k = 1, 2$, and 3. Nevertheless, s_1 is measured without the wave plates, s_2 when only the HWP is inserted with the fast axis at angle $\pi/8$ with respect to the horizontal, and s_3 when only the QWP is inserted with the fast axis at angle $\pi/4$ with respect to the horizontal. The 2×2 transformation matrices of the QWP and the HWP are given by [13]

$$\hat{U}_{\mathrm{QWP}}(\theta) = \frac{1}{\sqrt{2}}\begin{pmatrix} i + \cos(2\theta) & \sin(2\theta) \\ \sin(2\theta) & i - \cos(2\theta) \end{pmatrix}, \quad (4)$$

$$\hat{U}_{\mathrm{HWP}}(\theta) = \begin{pmatrix} \cos(2\theta) & \sin(2\theta) \\ \sin(2\theta) & -\cos(2\theta) \end{pmatrix}, \quad (5)$$

where θ is the angle between the fast axis and the horizontal. The effect of $\hat{U}_{\mathrm{HWP}}(\pi/8)$ is to convert $|D\rangle$ ($|A\rangle$) to $|H\rangle$ ($|V\rangle$), whereas for $\hat{U}_{\mathrm{QWP}}(\pi/4)$ the effect is to convert $|R\rangle$ ($|L\rangle$) to $|H\rangle$ ($|V\rangle$). Here, we define $|D\rangle = 1/\sqrt{2}(|H\rangle + |V\rangle)$, $|A\rangle = 1/\sqrt{2}(|H\rangle - |V\rangle)$, $|R\rangle = 1/\sqrt{2}(|H\rangle + i |V\rangle)$, and $|L\rangle = 1/\sqrt{2}(|H\rangle - i |V\rangle)$.

Similar to the derivation of the OPSPs in Eqs. (2a) to (3d), and based on the mathematical structure of the classical two-point Stokes parameters introduced in Ref. [15], the quantum generalization of these parameters can be defined under the present framework as

$$S_0 = \mathrm{Tr}[(|H, 0\rangle \langle H, 1| + |V, 0\rangle \langle V, 1|)\hat{\rho}] = \rho_{21} + \rho_{43}, \quad (6a)$$

$$S_1 = \mathrm{Tr}[(|H, 0\rangle \langle H, 1| - |V, 0\rangle \langle V, 1|)\hat{\rho}] = \rho_{21} - \rho_{43}, \quad (6b)$$

$$S_2 = \mathrm{Tr}[(|H, 0\rangle \langle V, 1| + |V, 0\rangle \langle H, 1|)\hat{\rho}] = \rho_{23} + \rho_{41}, \quad (6c)$$

$$S_3 = i\{\mathrm{Tr}[(|V, 0\rangle \langle H, 1| - |H, 0\rangle \langle V, 1|)\hat{\rho}]\} = i(\rho_{23} - \rho_{41}), \quad (6d)$$

which we call the TPSPs. While the OPSPs are real numbers, as a consequence of the hermiticity of the polarization-path density matrix, the TPSPs are generally complex and are obtained from correlations that involve photons propagating through both paths. In what follows we shall see how the TPSPs can be measured and their usefulness in realizing polarization-path state tomography.

III. POLARIZATION-PATH STATE TOMOGRAPHY

The results of Eqs. (2a) to (3d), together with Eqs. (6a) to (6d), allow us to rewrite the polarization-path matrix of Eq. (1) completely in terms of the OPSPs and TPSPs as follows:

$$\hat{\rho} = \frac{1}{2}\begin{pmatrix} s_0^{(0)} + s_1^{(0)} & S_0^* + S_1^* & s_2^{(0)} - is_3^{(0)} & S_2^* - iS_3^* \\ S_0 + S_1 & s_0^{(1)} + s_1^{(1)} & S_2 - iS_3 & s_2^{(1)} - is_3^{(1)} \\ s_2^{(0)} + is_3^{(0)} & S_2^* + iS_3^* & s_0^{(0)} - s_1^{(0)} & S_0^* - S_1^* \\ S_2 + iS_3 & s_2^{(1)} + is_3^{(1)} & S_0 - S_1 & s_0^{(1)} - s_1^{(1)} \end{pmatrix}. \quad (7)$$

This equation tells us that, given an ensemble of photons described by an unknown polarization-path density matrix, if
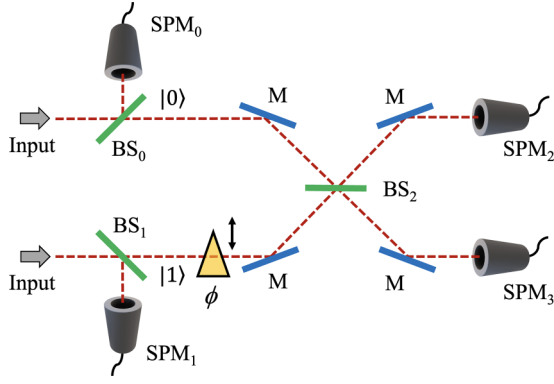
FIG. 2. Experimental setup to realize a complete polarization-path state tomography. Photons enter the setup in an arbitrary state of polarization and path. The 1:1 beam splitters BS_0 and BS_1 reflect part of the photons toward the SPM_0 and SPM_1 apparatuses to perform OPSP measurements, as depicted in Fig. 1. For the transmitted photons, an adjustable phase shift ϕ is applied in the lower path, after which the two paths are set as the input ports of the 1:1 beam splitter BS_2. Photons from the output ports are then collected by SPM_2 and SPM_3, which are used to obtain the TPSPs. The four M's represent perfectly reflecting mirrors.

we are able to measure the OPSPs and the TPSPs we can fully reconstruct the state. Therefore, the knowledge about these parameters allows us to realize polarization-path QST. To this end, we are left with the task of designing a way to assess the TPSPs.

In order to interpret the physical meaning of the four TPSPs, we first consider the experimental setup sketched in Fig. 2. It consists of single photons with arbitrary polarization entering the apparatus through the input paths $|0\rangle$ and $|1\rangle$, so that we can consider the general input state as described by the polarization-path density matrix as in Eq. (1). Initially, one half of the photons are reflected by two lossless 1:1 beam splitters, BS_0 and BS_1, on which measurements of the OPSPs can be made with SPM_0 and SPM_1, according to the scheme shown in Fig. 1. Since one half of all input photons are used to this end, in this case the OPSPs are identified according the relations $s_0 = 2(N_0 + N_1)/N_{in}$ and $s_k = 2(N_0 - N_1)/N_{in}$ with $k = 1, 2$, and 3. Here, N_{in} represents the total number of input photons in the experimental setup.

For the photons transmitted by BS_0 and BS_1, we have that those propagating along path 1 are subjected a controllable phase shift ϕ. Next, photons from both paths are superposed by a 1:1 lossless beam splitter BS_2, after which they follow toward SPM_2 and SPM_3. The effect of the phase shift is described by the operator $\hat{A} = |0\rangle \langle 0| + e^{i\phi} |1\rangle \langle 1|$ and the beam splitter is described by $\hat{B} = 1/\sqrt{2}(|0\rangle \langle 0| - |0\rangle \langle 1| + |1\rangle \langle 0| + |1\rangle \langle 1|)$ [20]. Together they cause the unitary transformation $\hat{U} = \hat{I}_p \otimes \hat{B}\hat{A}$, where $\hat{I}_p = |H\rangle \langle H| + |V\rangle \langle V|$ is the identity operator in the polarization Hilbert space. The corresponding transformation matrix is then given as

$$\hat{U} = \frac{1}{\sqrt{2}} \begin{pmatrix} 1 & -e^{i\phi} & 0 & 0 \\ 1 & e^{i\phi} & 0 & 0 \\ 0 & 0 & 1 & -e^{i\phi} \\ 0 & 0 & 1 & e^{i\phi} \end{pmatrix}. \tag{8}$$

After BS_2 the input state $\hat{\rho}$ is transformed into the final state $\hat{\rho}_f = \hat{U}\hat{\rho}\hat{U}^\dagger$. The calculation of $\hat{\rho}_f$ is straightforward, and the result is another polarization-path state represented in the basis $\{|H, 0\rangle; |H, 1\rangle; |V, 0\rangle; |V, 1\rangle\}$, but it is too lengthy to be written out explicitly. For $\hat{\rho}_f$ we have, for example, that the basis state $|H, 0\rangle$ ($|V, 1\rangle$) represents a horizontally (vertically) polarized photon in the optical mode which is collected by SPM_3 (SPM_2), and so on.

Next, with the procedure described in Fig. 1, the OPSPs for the state $\hat{\rho}_f$ in the paths $|0\rangle$ and $|1\rangle$ can be found. Given that one half of the input photons are transmitted by BS_0 and BS_1, these OPSPs must also be identified according to the relations $s_0 = 2(N_0 + N_1)/N_{in}$ and $s_k = 2(N_0 - N_1)/N_{in}$, with $k = 1, 2$, and 3. After some calculations, we can find that the OPSPs for the photons in path $|0\rangle$ (i.e., those collected by SPM_3) vary as a function of ϕ according to the relations:

$$s_{0f}^{(0)}(\phi) = \frac{1}{2}\big[s_0^{(0)} + s_0^{(1)} - 2\text{Re}(S_0 e^{i\phi})\big], \tag{9a}$$

$$s_{1f}^{(0)}(\phi) = \frac{1}{2}\big[s_1^{(0)} + s_1^{(1)} - 2\text{Re}(S_1 e^{i\phi})\big], \tag{9b}$$

$$s_{2f}^{(0)}(\phi) = \frac{1}{2}\big[s_2^{(0)} + s_2^{(1)} - 2\text{Re}(S_2 e^{i\phi})\big], \tag{9c}$$

$$s_{3f}^{(0)}(\phi) = \frac{1}{2}\big[s_3^{(0)} + s_3^{(1)} - 2\text{Re}(S_3 e^{i\phi})\big], \tag{9d}$$

where $\text{Re}(.)$ denotes the real part. Similarly, we can write the OPSPs as a function of ϕ for the photons in path $|1\rangle$ (i.e., those collected by SPM_2) as follows:

$$s_{0f}^{(1)}(\phi) = \frac{1}{2}\big[s_0^{(0)} + s_0^{(1)} + 2\text{Re}(S_0 e^{i\phi})\big], \tag{10a}$$

$$s_{1f}^{(1)}(\phi) = \frac{1}{2}\big[s_1^{(0)} + s_1^{(1)} + 2\text{Re}(S_1 e^{i\phi})\big], \tag{10b}$$

$$s_{2f}^{(1)}(\phi) = \frac{1}{2}\big[s_2^{(0)} + s_2^{(1)} + 2\text{Re}(S_2 e^{i\phi})\big], \tag{10c}$$

$$s_{3f}^{(1)}(\phi) = \frac{1}{2}\big[s_3^{(0)} + s_3^{(1)} + 2\text{Re}(S_3 e^{i\phi})\big]. \tag{10d}$$

We observe that, due to the unitarity of the interferometer transformation, the OPSPs obey a complementary relation:

$$s_n^{(0)} + s_n^{(1)} = s_{nf}^{(0)} + s_{nf}^{(1)}, \tag{11}$$

with $n = 0, 1, 2$, and 3. This relation, which holds for all values of ϕ, reflects the fact that there are no losses in the interferometer, and the degree of polarization of the photons is conserved.

At this point, we call attention to an important result obtained from Eqs. (9a) to (10d). The TPSPs quantify the contrast in the interference behavior of the OPSPs for the state $\hat{\rho}_f$ when ϕ is varied. A similar interpretation was also obtained in the classical context of Young's double-slit experiment [21]. This shows that by measuring the interference patterns of the OPSPs with the interferometer of Fig. 2, we can assess the TPSPs in a simple form. As we shall see, this will be useful to complete the characterization of the state $\hat{\rho}$. Let us first demonstrate in more detail how to obtain the TPSPs. We have that $\text{Re}(S_n e^{i\phi}) = \text{Re}(S_n)\cos\phi - \text{Im}(S_n)\sin\phi$, where $\text{Im}(.)$ denotes the imaginary part, with $n = 0, 1, 2$, and 3.

Therefore, to obtain the real and imaginary parts of the TPSPs, we only need to obtain the OPSPs along one of the path states of $\hat{\rho}_f$ for $\phi = 0$ and $\phi = \pi/2$. In considering path $|0\rangle$, from Eqs. (9a) to (9d) we find that

$$\mathrm{Re}(S_n) = \tfrac{1}{2}\big[s_n^{(0)} + s_n^{(1)}\big] - s_{nf}^{(0)}(0), \tag{12}$$

$$\mathrm{Im}(S_n) = -\tfrac{1}{2}\big[s_n^{(0)} + s_n^{(1)}\big] + s_{nf}^{(0)}(\pi/2). \tag{13}$$

From these two relations we can directly determine the TP-SPs, $S_n = \mathrm{Re}(S_n) + i\mathrm{Im}(S_n)$, which means that they can be determined through simple OPSP measurements. Additionally, in order to realize the state tomography with the least number of input photons, it is also important to get information about the TPSPs with the photons that propagate along path $|1\rangle$. From Eqs. (10a) to (10d), we find that

$$\mathrm{Re}(S_n) = -\tfrac{1}{2}\big[s_n^{(0)} + s_n^{(1)}\big] + s_{nf}^{(1)}(0), \tag{14}$$

$$\mathrm{Im}(S_n) = \tfrac{1}{2}\big[s_n^{(0)} + s_n^{(1)}\big] - s_{nf}^{(1)}(\pi/2). \tag{15}$$

This concludes our analysis of the QST applied to the two-qubit state encoded in the polarization and path DOF of a single photon.

Now, some important remarks are in order. First, we call attention to the fact that creating polarization-path entangled states in a single photon is straightforward [6,22]. For example, by passing a photon with diagonal polarization $|D\rangle$ through a PBS one generates the transformation $|D\rangle \rightarrow \frac{1}{\sqrt{2}}(|H, 0\rangle + |V, 1\rangle)$, which results in a single-photon maximally entangled state. On the other hand, the implementation of entangling gates for two qubits encoded in different photons is difficult because they do not interact directly, that is to say that it requires nonlinear couplings between photon paths [23]. Yet, we should note that to date entanglement involving different particles has found more significance in quantum technologies when compared to entanglement involving different DOF of a single particle [24]. Second, QST implementations typically require reconfigurations of the measurement apparatus in order to account for the many observables to be measured. Here, our QST proposal is realizable only with a single experimental setup. Indeed, we observe that the SPM scheme described in Fig. 1 can be rearranged to work without the need to insert or remove the wave plates when measuring different observables. In doing so, one must add a 2:1 beam splitter and a 1:1 beam splitter, together with two other PBS and two extra pairs of photodetectors, in the SPM apparatus (see Ref. [19]).

It is also important to mention here that sources of error have to be considered in the experimental setup of Fig. 2, e.g., the uncertainties in the angles of the wave plates used in the SPM. Errors in the experimental data provide a density matrix which may not correspond to a physical quantum state; i.e., the properties of unit trace or non-negativity may not be fulfilled. For this reason, methods of statistical inference to fix the obtained unphysical states have been employed, such as maximum likelihood estimation (MLE) [11] and Bayesian

inference [25]. The application of the MLE method for the reconstruction of a two-qubit state, which is the present case, is explored in Ref. [13]. This technique aims to find a physically plausible density matrix that maximizes the probability of obtaining the collected experimental data.

IV. CONCLUSIONS AND OUTLOOK

In conclusion, we have presented a QST method to read out the quantum state of two qubits encoded in the polarization and path DOF of a single photon. It consists of a single linear-optical setup in which all observables in the protocol can be assessed without the need of modifications in the apparatus. From the practical side, since the generation and control of polarization-path states are common tasks in quantum optical experiments [26], the tomographic reconstructions proposed here can represent an important step toward the application of such states in quantum technologies. From the theoretical side, we observed that the polarization-path density matrix can be completely characterized in terms of the OPSPs related to each of the two possible paths taken by the photon, which are real numbers, and the TPSPs, which are complex numbers that contain information about both the polarization and the coherence of the photon. This result, to a certain extent, reveals the role played by the two-point Stokes parameters in quantum optics.

As an outlook, given the increasing relevance of quantum optical experiments in simulating the behavior of open quantum systems [27–29], and the simplicity with which information can be encoded on the polarization and the path DOF of single photons, the QST protocol introduced here provides an accessible testbed for the study of the dynamics of open two-qubit systems [30–32]. Indeed, practical experimental studies of decoherence or entanglement loss can be realized by preparing an ensemble of photons in a well-defined polarization-path state, passing them through the environment in question, and then reading out the output state with the setup described in Fig. 2. In addition, with optical simulations of quantum thermodynamic processes, it is also possible to describe a qubit system interacting with decohering and thermalizing environments by manipulation of the polarization and the path DOF of the photons [33,34]. Such simulations have significantly broadened our understanding about how coherence and system-environment quantum correlations affect the behavior of nonequilibrium quantum dynamics [35–37]. In this perspective, our QST technique for the reconstruction of single-photon polarization-path states can provide an extra tool for an even more detailed understanding of such processes.

[1] C. H. Bennett and S. J. Wiesner, Communication via one- and two-particle operators on Einstein-Podolsky-Rosen states, Phys. Rev. Lett. **69**, 2881 (1992).

[2] R. Raussendorf and H. J. Briegel, A one-way quantum computer, Phys. Rev. Lett. **86**, 5188 (2001).

[3] A. K. Ekert, Quantum cryptography based on Bell's theorem, Phys. Rev. Lett. **67**, 661 (1991).

[4] C. H. Bennett, G. Brassard, C. Crépeau, R. Jozsa, A. Peres, and W. K. Wootters, Teleporting an unknown quantum state via dual classical and Einstein-Podolsky-Rosen channels, Phys. Rev. Lett. **70**, 1895 (1993).

[5] C. Couteau, S. Barz, T. Durt, T. Gerrits, J. Huwer, R. Prevedel, J. Rarity, A. Shields, and G. Weihs, Applications of single photons to quantum communication and computing, Nat. Rev. Phys. **5**, 326 (2023).

[6] P. Kok, W. J. Munro, K. Nemoto, T. C. Ralph, J. P. Dowling, and G. J. Milburn, Linear optical quantum computing with photonic qubits, Rev. Mod. Phys. **79**, 135 (2007).

[7] A. Mair, A. Vaziri, G. Weihs, and A. Zeilinger, Entanglement of the orbital angular momentum states of photons, Nature (London) **412**, 313 (2001).

[8] I. Marcikic, H. de Riedmatten, W. Tittel, H. Zbinden, M. Legré, and N. Gisin, Distribution of time-bin entangled qubits over 50 km of optical fiber, Phys. Rev. Lett. **93**, 180502 (2004)

[9] Y. Pilnyak, P. Zilber, L. Cohen, and H. S. Eisenberg, Quantum tomography of photon states encoded in polarization and picosecond time bins, Phys. Rev. A **100**, 043826 (2019).

[10] G. M. D'Ariano, M. G. Paris, and M. F. Sacchi, Quantum tomography, Adv. Imaging Electron Phys. **128**, 205 (2003).

[11] A. I. Lvovsky and M. G. Raymer, Continuous-variable optical quantum-state tomography, Rev. Mod. Phys. **81**, 299 (2009).

[12] E. Toninelli, B. Ndagano, A. Vallés, B. Sephton, I. Nape, A. Ambrosio, F. Capasso, M. J. Padgett, and A. Forbes, Concepts in quantum state tomography and classical implementation with intense light: A tutorial, Adv. Opt. Photonics **11**, 67 (2019).

[13] D. F. V. James, P. G. Kwiat, W. J. Munro, and A. G. White, Measurement of qubits, Phys. Rev. A **64**, 052312 (2001).

[14] Y. Hasegawa, R. Loidl, G. Badurek, S. Filipp, J. Klepp, and H. Rauch, Evidence for entanglement and full tomographic analysis of Bell states in a single-neutron system, Phys. Rev. A **76**, 052108 (2007).

[15] O. Korotkova and E. Wolf, Generalized Stokes parameters of random electromagnetic beams, Opt. Lett. **30**, 198 (2005).

[16] B. de Lima Bernardo, Unified quantum density matrix description of coherence and polarization, Phys. Lett. A **381**, 2239 (2017).

[17] A. F. dos Santos, N. E. L. Barbosa, J. L. M. Ferreira, and B. L. Bernardo, Influence of polarization and the environment on wave-particle duality, Quant. Inf. Process. **22**, 63 (2023).

[18] J. B. Altepeter, D. F. V. James, and P. G. Kwiat, in *Quantum State Estimation* (Springer, Berlin, 2004).

[19] O. Bayraktar, M. Swillo, C. Canalias, and G. Björk, Quantum-polarization state tomography, Phys. Rev. A **94**, 020105(R) (2016).

[20] M. A. Nielsen and I. L. Chuang, *Quantum Computation and Quantum Information* (Cambridge University, Cambridge, England, 2010).

[21] T. Setälä, J. Tervo, and A. T. Friberg, Stokes parameters and polarization contrasts in Young's interference experiment, Opt. Lett. **31**, 2208 (2006).

[22] B.-G. Englert, C. Kurtsiefer, and H. Weinfurter, Universal unitary gate for single-photon two-qubit states, Phys. Rev. A **63**, 032303 (2001).

[23] E. Knill, R. Laflamme, and G. J. Milburn, A scheme for efficient quantum computation with linear optics, Nature (London) **409**, 46 (2001).

[24] M. Erhard, M. Krenn, and A. Zeilinger, Advances in high dimensional quantum entanglement, Nat. Rev. Phys. **2**, 365 (2020).

[25] J. M. Lukens, K. J. H. Law, A. Jasra, and P. Lougovski, A practical and efficient approach for Bayesian quantum state estimation, New J. Phys. **22**, 063038 (2020).

[26] P. Kok and B. W. Lovett, *Introduction to Optical Quantum Information Processing* (Cambridge University, Cambridge, England, 2010).

[27] B.-H. Liu, L. Li, Y.-F. Huang, C.-F. Li, G.-C. Guo, E. M. Laine, H.-P. Breuer, and J. Piilo, Experimental control of the transition from Markovian to non-Markovian dynamics of open quantum systems, Nat. Phys. **7**, 931 (2011).

[28] M. D. Vidrighin, O. Dahlsten, M. Barbieri, M. S. Kim, V. Vedral, and I. A. Walmsley, Photonic Maxwell's demon, Phys. Rev. Lett. **116**, 050401 (2016).

[29] F. H. B. Somhorst *et al.*, Quantum simulation of thermodynamics in an integrated quantum photonic processor, Nat. Commun. **14**, 3895 (2023).

[30] C. Viviescas, I. Guevara, A. R. R. Carvalho, M. Busse, and A. Buchleitner, Entanglement dynamics in open two-qubit systems via diffusive quantum trajectories, Phys. Rev. Lett. **105**, 210502 (2010).

[31] E. Ghasemian and M. K. Tavassoly, Generation of Werner-like states via a two-qubit system plunged in a thermal reservoir and their application in solving binary classification problems, Sci. Rep. **11**, 3554 (2021).

[32] O. Siltanen, T. Kuusela, and J. Piilo, Distributing memory effects in an open two-qubit system, Phys. Rev. A **102**, 022225 (2020).

[33] G. H. Aguilar, A. Valdés-Hernández, L. Davidovich, S. P. Walborn, and P. H. S. Ribeiro, Experimental entanglement redistribution under decoherence channels, Phys. Rev. Lett. **113**, 240501 (2014).

[34] K. Khan, W. F. Magalhães, J. S. Araújo, B. L. Bernardo, and G. H. Aguilar, Quantum coherence and the principle of microscopic reversibility, Phys. Rev. A **108**, 052215 (2023).

[35] L. Mancino, M. Sbroscia, I. Gianani, E. Roccia, and M. Barbieri, Quantum simulation of single-qubit thermometry using linear optics, Phys. Rev. Lett. **118**, 130502 (2017).

[36] M. Bellini, H. Kwon, N. Biagi, S. Francesconi, A. Zavatta, and M. S. Kim, Demonstrating quantum microscopic reversibility using coherent states of light, Phys. Rev. Lett. **129**, 170604 (2022).

[37] K. Khan, J. S. Araújo, W. F. Magalhães, G. H. Aguilar, and B. L. Bernardo, Coherent energy fluctuation theorems: Theory and experiment, Quantum Sci. Technol. **7**, 045010 (2022).